Two ions in a Penning trap: Implications for precision mass spectroscopy

Eric A. Cornell,* Kevin R. Boyce, Deborah L. K. Fygenson,† and David E. Pritchard
Research Laboratory of Electronics, Department of Physics, Massachusetts Institute of Technology, Cambridge, Massachusetts 02139
(Received 22 March 1991; revised manuscript received 23 September 1991)

With the goal of increasing the accuracy of Penning-trap mass spectroscopy to a part in 10^{11}, we model the motion of two simultaneously trapped, dissimilar ions. Simultaneous cyclotron resonance on two trapped ions will circumvent the problem of temporal instability in the trapping fields. Conservation of energy and canonical angular momentum require that, in the regime appropriate for mass spectroscopy, the average interion spacing be an approximate constant of the motion. Cyclotron-frequency perturbation from ion-ion repulsion is therefore limited. Orbits that minimize measurement errors from residual field imperfections are shown to be both stable and attainable. Experimental results demonstrating the simultaneous trapping of a single N_2^+ ion and a single CO^+ ion are presented.

PACS number(s): 07.75.+h, 32.80.Pj, 46.10.+z, 41.90.+e

I. INTRODUCTION

The most accurate comparisons of ion masses are currently performed in Penning traps [1–3] by alternately loading the two ion species being compared. The trap is loaded with a few ions, or even a single ion of one species; its cyclotron frequency is determined; the ion is replaced with a second species; and the new cyclotron frequency is determined. With corrections for various trap perturbations, the ratio of the cyclotron frequencies is simply the inverse of the mass ratio. Sequential-measurement technique has progressed to the point where mass ratios may now be determined to better than a part in 10^9, but further improvement in accuracy must surmount a formidable technical obstacle—temporal instability in the magnetic field at the site of the ions. While the trapped species are being exchanged, any unpredictable changes in the magnetic field introduce random errors in the measured mass ratio. Let us take as an example an ammonia mass doublet ($^{15}NH_3^+$ and $^{14}NDH_2^+$) whose masses differ by about 5 parts in 10^4. To make a major impact in fundamental-constant work [4], the mass ratio must be determined to a part in 10^{11}. A traditional sequential measurement must determine each ion's cyclotron frequency to tens of microhertz out of 7 MHz. While the ions are being exchanged, the drift in the magnetic field must be known to a part in 10^{11} over an hour or more. Also draconian is the requirement on electric-field stability [5]: 2 parts in 10^8.

On the other hand, if the two ions are measured simultaneously, in the same trap, the requirements on both electric- and magnetic-field stability relax immensely. As we shall see in Sec. IV, to compare the masses in a mass doublet the only quantity that has to be measured to really high precision is the instantaneous cyclotron-frequency difference, which is relatively insensitive to field drift. The magnetic field must be constant only to parts in 10^8, the electric field only to a part in 10^4, both standards already achieved in our apparatus. (An alternate route to higher accuracy involves improved stabilization of the trapping fields. For example, Van Dycke *et al.* [6] and Gabrielse and Tan [7] have shown that the region at the center of the trapping magnet can be shielded from fluctuation in ambient fields by savvy design of superconducting coils.)

Although simultaneous two-ion cyclotron resonance resolves the problem of temporal field drifts, it raises new problems. If the two ions are too close together in the trap, the Coulombic coupling may perturb their cyclotron frequencies unacceptably. On the other hand, if the ions are well spaced, any residual spatial inhomogeneity of the trapping fields may affect the two ions unequally. The point of our paper is to examine the motion of two, simultaneously trapped ions, with emphasis on the implications for precision mass spectroscopy. As far as we know, our work is the first to examine carefully the Penning-trap motion of two ions in the well-separated, "orderly" regime.

II. BASIC TWO-ION MOTION

The ideal Penning trap [8] consists of a strong, uniform magnetic field, and a quadrupole electric field, usually established by three electrodes, all hyperbolas of rotation (Fig. 1). We write the electric and magnetic fields in cylindrical coordinates as

$$\mathbf{E}(\rho,z)=(V_t/d^2)(\rho\hat{\boldsymbol{\rho}}/2-z\hat{\mathbf{z}}) ,$$
$$\mathbf{B}=B\hat{\mathbf{z}} ,$$

where V_t is the potential between the ring electrode and the endcap electrodes and d is the characteristic trap size, defined in Fig. 1. In the ideal fields, the equation of motion is linear and is readily solved to yield three normal modes, known as the axial, the magnetron, and the trap cyclotron modes [9]. The frequencies are, respectively,

$$\omega_z=[eV_t/(md^2)]^{1/2} ,$$
$$\omega_m=[\omega_c-(\omega_c^2-2\omega_z^2)^{1/2}]/2 ,$$
$$\omega_c'=[\omega_c+(\omega_c^2-2\omega_z^2)^{1/2}]/2 ,$$

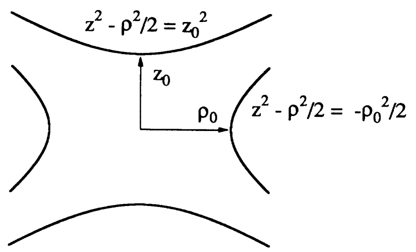

FIG. 1. The geometry of the Penning trap. The electrodes are hyperbolic surfaces of rotation. In our trap, $\rho_0=0.696$ cm and $z_0=0.600$ cm, giving an effective trap size $d\equiv(\rho_0^2/4+z_0^2/2)^{1/2}=0.549$ cm.

where ω_c is the free-space cyclotron frequency; $\omega_c=eB/(mc)$. We refer to the magnitudes of the normal mode motions as the mode radii, denoted, respectively, by a_z, ρ_m, and ρ_c. The trap cyclotron mode is so named because in the limit of vanishing electric fields the trap cyclotron frequency approaches the free-space cyclotron frequency. For precision mass spectroscopy in a Penning trap, the electric field is always weak enough that $\omega_c' \gg \omega_z \gg \omega_m$.

The motion of two ions in a Penning trap is a three-body problem and in general cannot be solved exactly. However, in the regime of experimental interest we can make several useful approximations. If the initial ion-ion separation ρ_s is large enough to keep the ion-ion coupling weak, we can carry over from the single-ion solution the idea of independent cyclotron and axial motions for each ion. Ion-ion interaction will perturb the frequencies of these four modes, to be sure, but we will not have to think of the axial or cyclotron motions as collective modes of the two ions.

The magnetron motion, however, is another story. The unperturbed magnetron frequencies of a mass doublet are so nearly degenerate that even a small perturbation will strongly couple the magnetron modes. We will use conservation principles to establish that the distance between the two ions—an important quantity that sets the scale of ion-ion perturbations—is an approximate constant of the motion. Further, we will show that the geometry of the locked magnetron motion is such that, over time, the ions sample very similar fields.

A. Conserved quantities

Regardless of the number of ions in the trap, the total energy and the z component of the total canonical angular momentum [10] are conserved quantities. As a first pass at the problem of two-ion motion, let us imagine that the axial and the cyclotron radii of both ions are zero, and write the energy and canonical angular momentum in the Coulomb gauge as

$$E=\frac{-eV_t}{4d^2}(\rho_1^2+\rho_2^2)+\frac{e^2}{\rho_s}+\tfrac{1}{2}m_1(\dot{\boldsymbol{\rho}}_1)^2+\tfrac{1}{2}m_2(\dot{\boldsymbol{\rho}}_2)^2\ , \tag{2.1}$$

$$\mathbf{L}=L_z\hat{\mathbf{z}}=\frac{e\hat{\mathbf{B}}}{2c}(\rho_1^2+\rho_2^2)+m_1\boldsymbol{\rho}_1\times\dot{\boldsymbol{\rho}}_1+m_2\boldsymbol{\rho}_2\times\dot{\boldsymbol{\rho}}_2\ , \tag{2.2}$$

where $\boldsymbol{\rho}_s\equiv\boldsymbol{\rho}_1-\boldsymbol{\rho}_2$ is the ion-ion separation [Fig. 2(a)]. Here, and throughout the paper, the subscripts 1 and 2 refer to properties of one ion or the other, and the subscript 0 refers to properties of a hypothetical ion whose mass is the average of the masses of the two ions. We now rewrite the equations, explicitly separating out the effects of the ion-ion perturbation:

$$E=\rho_1^2\left[\frac{-eV_t}{4d^2}+\frac{m_1\omega_{m1}^2}{2}\right]+\rho_2^2\left[\frac{-eV_t}{4d^2}+\frac{m_2\omega_{m2}^2}{2}\right]+\frac{e^2}{\rho_s}+S_{KE}\ , \tag{2.3}$$

$$L_z=\rho_1^2\left[\frac{eB}{2c}-m_1\omega_{m1}\right]+\rho_2^2\left[\frac{eB}{2c}-m_2\omega_{m2}\right]+S_L\ , \tag{2.4}$$

where we have substituted for the ion velocities the values of their unperturbed magnetron velocities: $\dot{\boldsymbol{\rho}}_i=-\omega_{mi}\hat{\mathbf{z}}\times\boldsymbol{\rho}_i$. The small errors associated with this substitution are accounted for in the terms S_{KE} and S_L (for small bit of kinetic energy and of angular momentum, respectively). The ion-ion interaction is represented only by a potential term, e^2/ρ_s, and by the two small corrections S_{KE} and S_L. We now make two key approximations (whose validity we will verify shortly): first, that

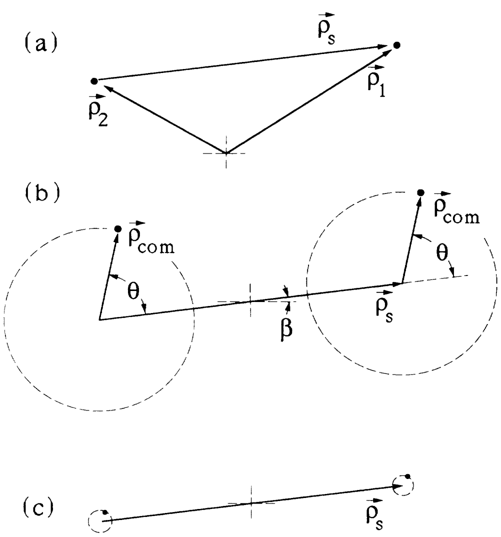

FIG. 2. The magnetic field comes up out of the plane of the figure. (a) When only the magnetron motions are considered, the angular momentum and energy of the system of two particles are well approximated by functions only of the distances $\rho_1=|\boldsymbol{\rho}_1|$, $\rho_2=|\boldsymbol{\rho}_2|$, and $\rho_s=|\boldsymbol{\rho}_s|$. (b) Any initial positions of ions 1 and 2 can be described as superpositions of the common-mode vector $\boldsymbol{\rho}_{\rm com}$ and the separation vector $\boldsymbol{\rho}_s$. Both vectors rotate clockwise. In a frame rotating at ω_s, the ions trace out counterclockwise tandem circles centered on opposite sides of the origin. The angular frequency of the motion is $\omega_s-\omega_{\rm com}$. (c) If the common-mode motion is cooled, the ions are "parked" in orbits on either side of the origin. This configuration ensures that, as the ions move around the trap center, they sample very-nearly-identical annular rings, thus minimizing the amount by which spatial inhomogeneities in the trapping fields affect the measured frequency mass ratio.

$\omega_{m1}=\omega_{m2}=\omega_{m0}$, and second, that $S_{KE}=S_L=0$. Defining a mass splitting η such that $m_1=m_0(1+\eta)$ and $m_2=m_0(1-\eta)$, we rewrite the energy and angular momentum:

$$\frac{E}{m_0}-\frac{e^2}{m_0\rho_s}=(\rho_1^2+\rho_2^2)\left[\frac{-\omega_{z0}^2}{4}+\frac{\omega_{m0}^2}{2}\right]+(\rho_1^2-\rho_2^2)\left[\frac{\eta\omega_{m0}^2}{2}\right], \quad (2.5)$$

$$\frac{L_z}{m_0}=(\rho_1^2+\rho_2^2)(\omega_{c0}/2-\omega_{m0})+(\rho_1^2-\rho_2^2)(-\eta\omega_{m0}) . \quad (2.6)$$

ρ_1 and ρ_2 evolve over time, but conservation of energy and angular momentum put a strict limit on the amount ρ_s can change. In order to conserve L_z, changes in ρ_1^2 and in ρ_2^2 must be related. Equation (2.6) gives

$$\delta(\rho_1^2+\rho_2^2)=\frac{2\eta\omega_{m0}}{\omega_{c0}-2\omega_{m0}}\delta(\rho_1^2-\rho_2^2) . \quad (2.7)$$

We will simplify expressions using the inequality $\omega_c >> \omega_z >> \omega_m$. (In practice, the ratio is about 8000:160:1.6 for a mass-18 ion.) Combining Eqs. (2.5) and (2.7) and making use of the approximation $\omega_m \approx \omega_z^2/(2\omega_c)$, we find that changes in the ion-ion potential energy are restricted:

$$\delta\left[\frac{e^2}{m_0\rho_s}\right]=\frac{\eta\omega_{m0}^2}{2}\delta(\rho_1^2-\rho_2^2) . \quad (2.8)$$

And what, typically, is the maximum expected change in $(\rho_1^2-\rho_2^2)$? As we shall see in Sec. III, ions are typically loaded into the trap with an initial separation $\rho_s=2\rho_{\rm com}$, where $\rho_{\rm com}$ is the length of the average position vector,

$$\boldsymbol{\rho}_{\rm com}=(\boldsymbol{\rho}_1+\boldsymbol{\rho}_2)/2 .$$

Further, as we shall see below, both ρ_s and $\rho_{\rm com}$ are approximate constants of the motion. The maximum change in $(\rho_1^2-\rho_2^2)$ we can expect then is about $2\rho_s^2$, which implies that the maximum possible change in ρ_s is

$$\frac{\delta\rho_s}{\rho_s}=\frac{\eta\omega_{m0}^2}{\Omega^2} , \quad (2.9)$$

where we have defined the coupling constant

$$\Omega=(e^2/m_0\rho_s^3)^{1/2} . \quad (2.10)$$

In the limit of degenerate masses (η goes to 0), the ion-ion separation ρ_s is a constant of the motion. ρ_s remains an approximate constant of the motion as long as the mass splitting is small compared to the coupling, $\eta \ll \Omega^2/\omega_{m0}^2$.

We will look more carefully at the effects of nondegenerate masses on the orbits in Sec. IV below, but for now we keep $\eta=0$ and make the purely geometrical observation [11] that since ρ_s and $\rho_1^2+\rho_2^2$ are both constant, so must be $\rho_{\rm com}$. The allowed ion motions thus decompose nicely into a common mode and a "stretch" mode [Fig. 2(b)]. The stretch mode is so called in analogy with tightly coupled harmonic oscillators, although of course in this case a vector pointing from one ion to the other does not stretch in length but merely rotates.

Let us recheck our earlier assumptions for self-consistency. First, how large are the supposedly small terms S_{KE} and S_L and how much did neglecting them affect the calculated length of the vectors $\rho_{\rm com}$ and ρ_s? Because the ions are in a strong magnetic field, the electric field from each ion induces an E-cross-B drift in the other. These drifts are relatively small corrections to the unperturbed ion velocities, and (for the magnetron motion) the velocity terms are in turn relatively much smaller than the electric and magnetic potential contributions to the total angular momentum and total energy. The magnitude of the E-cross-B velocity is $cE_{\text{ion-ion}}/B$, or $ec/(B\rho_s^2)$. The largest change that this drift could cause in the angular momentum would be if the induced drift were perpendicular to the ion's position vector $\boldsymbol{\rho}_i$ and if that vector were at its maximum length. Given the typical experimental initial conditions mentioned above, $\rho_i \le \rho_s$, so that the change in angular momentum must be less than

$$\delta S_L=m_0ce/(B\rho_s)=m_0\rho_s^2(\Omega^2/\omega_{c0}) . \quad (2.11)$$

Similarly, the maximum change in the kinetic energy occurs when the drift velocity is adding to or subtracting from the ion's maximum velocity. The maximum possible change in the kinetic energy is then

$$\delta S_{KE}=m_0\rho_s^2(\omega_{m0}/\omega_{c0})\Omega^2 .$$

Reinserting the maximum values δS_L and δS_{KE} back into the the conservation equations [(2.5) and (2.6)] from which they were discarded, we rewrite Eqs. (2.7) and (2.8), this time indicating the order of the error associated with the approximation:

$$\frac{\delta(\rho_1^2+\rho_2^2)}{\rho_s^2}=\frac{2\eta\omega_{m0}}{\omega_{c0}-2\omega_{m0}}\frac{\delta(\rho_1^2-\rho_2^2)}{\rho_s^2}+O\left[\frac{\Omega^2}{\omega_{c0}^2}\right], \quad (2.12)$$

$$\frac{\delta\rho_s}{\rho_s}=\frac{-\eta\omega_{m0}^2}{2\Omega^2}\frac{\delta(\rho_1^2-\rho_2^2)}{\rho_s^2}+O\left[\frac{\omega_{z0}^2}{\omega_{c0}^2}\right] . \quad (2.13)$$

It is easy to verify that the errors in ρ_s and $\rho_{\rm com}$ associated with our other major approximation, $\omega_{m1}\approx\omega_{m2}\approx\omega_{m0}$, are smaller still. The errors in the results obtained so far in this section are thus small as long as $\omega_{z0}^2 \ll \omega_{c0}^2$, $\Omega^2 \ll \omega_{c0}^2$, and $\eta\omega_m^2 \ll \Omega^2$. These inequalities are all experimentally realizable. With the reasonable initial value of $\rho_s=0.10$ cm, we have in our trap for the ammonia example previously cited, $\Omega^2=8\times10^6$, $\eta\omega_m^2/\Omega^2=4\times10^{-3}$, $\Omega^2/\omega_{c0}^2=4\times10^{-9}$, and $\omega_{z0}^2/\omega_{c0}^2=5\times10^{-4}$.

B. Locked motion

Having established the geometry of the modes (or approximated them, in the more realistic case of nondegenerate masses) by the use of conservation principles, we can confidently solve the equations of motion for the corresponding frequencies. The equations of motion for two particles moving in the midplane of a Penning trap are

$$m_1\ddot{\boldsymbol{\rho}}_1=\frac{eB}{c}\dot{\boldsymbol{\rho}}_1\times\hat{\mathbf{z}}+\frac{eV_t}{2d^2}\boldsymbol{\rho}_1+\frac{e^2(\boldsymbol{\rho}_1-\boldsymbol{\rho}_2)}{|\boldsymbol{\rho}_1-\boldsymbol{\rho}_2|^3}\ , \tag{2.14}$$

$$m_2\ddot{\boldsymbol{\rho}}_2=\frac{eB}{c}\dot{\boldsymbol{\rho}}_2\times\hat{\mathbf{z}}+\frac{eV_t}{2d^2}\boldsymbol{\rho}_2-\frac{e^2(\boldsymbol{\rho}_1-\boldsymbol{\rho}_2)}{|\boldsymbol{\rho}_1-\boldsymbol{\rho}_2|^3}\ . \tag{2.15}$$

These equations are linear except for the cubic in the denominator of the interaction term. We use the result of our conservation-principle argument, $|\boldsymbol{\rho}_1-\boldsymbol{\rho}_2|=\rho_s\approx$const, to eliminate the nonlinear term. Dividing though by m_0, we get the equations

$$\begin{aligned}(1+\eta)\ddot{\boldsymbol{\rho}}_1&=\omega_{c0}\dot{\boldsymbol{\rho}}_1\times\hat{\mathbf{z}}+(\omega_{z0}^2/2)\boldsymbol{\rho}_1+\Omega^2(\boldsymbol{\rho}_1-\boldsymbol{\rho}_2)\ ,\\(1-\eta)\ddot{\boldsymbol{\rho}}_2&=\omega_{c0}\dot{\boldsymbol{\rho}}_2\times\hat{\mathbf{z}}+(\omega_{z0}^2/2)\boldsymbol{\rho}_2-\Omega^2(\boldsymbol{\rho}_1-\boldsymbol{\rho}_2)\ .\end{aligned} \tag{2.16}$$

These coupled linear equations are exactly solvable. We get that the two normal-mode magnetron frequencies are

$$\begin{aligned}\omega_{\rm com}&=\omega_{m0}-O((\eta^2\omega_{m0}^4)/(\Omega^2\omega_{c0}))\ ,\\\omega_s&=\omega_{m0}+2\Omega^2/\omega_{c0}+O((\eta^2\omega_{m0}^4)/(\Omega^2\omega_{c0}))\ .\end{aligned} \tag{2.17}$$

In the limit of nearly degenerate masses, $\eta\omega_m^2/\Omega^2\ll 1$, the normal-mode motions correspond to clockwise motion of the vectors shown in Fig. 2(b). (The small corrections to the geometry of the modes for nondegenerate mass are described in Sec. IV.)

Viewed in a frame rotating at ω_s, the ions appear to drift in tandem counterclockwise around twin circles centered on either side of the trap center [Fig. 2(b)]. The ions take turns moving nearer to and further from trap center, with a period of motion

$$t_e=2\pi/(\omega_s-\omega_{\rm com})=\pi\omega_{c0}/\Omega^2\ ,$$

perhaps 15 sec.

From the point of view of the precision mass spectroscopist, this tandem motion is very welcome. If its period is short compared to the time between the pulses of a separated oscillatory field (SOF) resonance measurement, the ions' orbits will average away, albeit incompletely, the effects of field inhomogeneities that are functions of distance from trap center. It would be better yet if $\rho_{\rm com}$ were shrunk as much as possible while ρ_s remained relatively large [Fig. 2(c)]. In such a configuration the two ions would follow each other around and around the center of the trap, sampling almost exactly the same fields. The specific cooling of $\rho_{\rm com}$ can be accomplished by an extension of the standard axial-sideband-cooling technique [12,13]. We will discuss this in detail in a future publication.

C. Axial motion

Now that we understand the basic principles of locked magnetron motion, we relax the requirement that the axial and cyclotron radii vanish. $\boldsymbol{\rho}_s$ and $\boldsymbol{\rho}_{\rm com}$ are no longer determined from the instantaneous ion positions, but from the guiding centers of each ion's axial-cyclotron motion. We require that the cyclotron radii ρ_{c1} and ρ_{c2} be small enough to avoid the possibility of a hard collision, that is, that $\rho_{c1}+\rho_{c2}<\rho_s$. The ion-ion potential averaged over the cyclotron and axial motion is no longer simply e^2/ρ_s, but is now a function of the cyclotron and axial radii as well as ρ_s. However, as long as the inter-ion potential [the quantity that appears in parentheses on the left-hand side of Eq. (2.8)] is a monotonic function of ρ_s, the result that ρ_s and $\rho_{\rm com}$ are constants of the motion remains valid. In the absence of hard collisions, the large separation between the mode frequencies ensures that energy and momentum will not be transferred from axial and cyclotron modes to the magnetron motion.

If the axial displacements z_1 and z_2 are small compared to ρ_s, then we can expand the axial component of the ion-ion repulsive force, keeping only the dipole term which is linear in z_1-z_2:

$$\begin{aligned}F_{z1}&=e^2(z_1-z_2)/[(z_1-z_2)^2+\rho_s^2]^{3/2}\ ,\\F_{z1}&=-F_{z2}\approx m_0\Omega^2(z_1-z_2)\quad\text{for } |z_1-z_2|\ll\rho_s\ .\end{aligned} \tag{2.18}$$

Assuming a weak coupling, that is, $\Omega^2\ll|\omega_z^2\eta|$ (for the example of the ammonia ions already discussed, $\rho_s=0.06$ cm gives $\Omega^2/|\omega_{z0}^2\eta|=0.13$), we get for the axial frequencies

$$\omega_{z1}'-\omega_{z1}=\frac{-\Omega^2}{2\omega_{z0}}-\frac{\Omega^2}{2\omega_{z0}}\left[\frac{\Omega^2}{2\eta\omega_{z0}^2}\right]+\cdots\ , \tag{2.19}$$

$$\omega_{z2}'-\omega_{z2}=\frac{-\Omega^2}{2\omega_{z0}}+\frac{\Omega^2}{2\omega_{z0}}\left[\frac{\Omega^2}{2\eta\omega_{z0}^2}\right]+\cdots\ . \tag{2.20}$$

The primed variables here refer to the frequencies shifted by the ion-ion perturbation. As long as the axial coupling is weak, $\Omega^2/(\eta\omega_z^2)\ll 1$, the perturbations are very nearly symmetric, that is, the axial difference frequency $(\omega_{z1}'-\omega_{z2}')$ is not significantly perturbed.

In experimentally realizable situations the dipole approximation $(z_1-z_2)\ll\rho_s$ may not be valid. To obtain an adequate signal-to-noise ratio in the axial motion detector, the ions may well have to be driven to axial motion with peak amplitudes a_{z1} and $a_{z2}>\rho_s$. In this case, the coupling is nonlinear and Ω is replaced with an effective coupling Ω', which depends on the amplitudes a_{z1} and a_{z2} and which is always less than Ω. As the axial motions damp, Ω' increases and the frequencies shift. The signals detected after exciting the axial motion will thus be "chirped." However, if the axial amplitudes remain equal to each other as the ions damp, the perturbation remains symmetric, and the frequency difference $\omega_{z1}'-\omega_{z2}'$ will be only slightly perturbed.

We have established in this section a general picture of two-ion dynamics in an experimentally interesting regime, with magnetron modes of the ions tightly locked into coordinated motion and with the axial modes perturbed in frequency but still independent. Ion-ion perturbation of the cyclotrons frequencies, and other topics in two-ion motion germane to precision mass spectroscopy, will be covered in Sec. IV.

III. PRELIMINARY TWO-ION EXPERIMENTS

We describe in this section our preliminary experimental work on two-ion trapping [14]. The work demonstrates techniques for loading a single ion of each of two species into the trap and shows that, with appropriate initial interion spacing, the axial motion of the two ions is well behaved. We have worked with the doublet CO^+-N_2^+, whose masses differ by about 4 parts in 10^4. The apparatus, described in Refs. [2] and [15], is a Penning trap in ultrahigh vacuum at 4.2 K, in an 8.5-T magnetic field. When the ions are tuned to be resonant with our axial motion detector, the axial frequencies of the two ion species differ by 33 Hz out of about 160 kHz.

A pair of ions is loaded as follows: From a room-temperature gas-handling manifold we admit a small pulse of N_2 gas, which drifts down into the cryogenic portion of the apparatus and through a hole in the upper endcap into the trap volume, where it encounters a beam of electrons injected from below the trap. The average number of ions produced by electron collisions is proportional to the product of the electron current and the number of molecules injected. This product has been calibrated [14] to produce, on the average, $\frac{1}{2}$ ion with every gas pulse admitted. After each pulse of gas, we test for ions by driving the lower endcap and looking for the signal from the axially excited ion. Occasionally, more than one ion is trapped, in which case we dump the trap and start again. It rarely takes more than a few attempts to catch a single N_2^+ ion.

Because the ionizing electron beam is thin and very nearly coaxial with the trap, ions are initially created near the axis of the trap, i.e., with a small magnetron radius. The moment the second ion is created, the ion-ion separation ρ_s will be a constant of the motion. Thus if we wish the two-ion motion to have a particular ρ_s, we must control how far the initially created N_2^+ ion is from the site of the CO ionization. Before loading the CO^+ ion, we drive the magnetron motion of the newly trapped single N_2^+ ion to about 0.06 cm, using a short resonant pulse at the magnetron frequency. (The minimum radius of the center trap electrode is 0.7 cm.) Then we proceed as with N_2 to trap a single CO^+ ion. At the moment the CO^+ ion is created (at trap center), the N_2 ion is 0.06 cm from trap center. Thus initial ρ_s is 0.06 cm, and initial ρ_{com} is 0.03 cm.

When we load the second ion without preparing the first in a large magnetron orbit, the ions are created with $\rho_{com} \cong \rho_s < 0.02$ cm. The axial signal detected under these conditions is very irreproducible. Sometimes a component of the axial signal appears at the average of the two unperturbed frequencies, and sometimes (especially when the ions are driven hard) we see individual signals in the neighborhood of the unperturbed frequencies. With the radial separation so small, the approximations of Sec. II are not valid, and it is hard to predict what sort of motion should occur. In any case this close-spaced configuration is not appropriate for precision metrology and the remainder of the measurements described in this section were performed on ions radially spaced by about 0.06 cm.

Truly simultaneous resonance measurements on the two ions require the ability to detect both ions simultaneously. Although the ions' axial-frequency splitting, 33 Hz, is much larger than the effective bandwidth of our detector, we use a trick to bring components of both signals within the bandwidth of the detector simultaneously. Adding a small ac term to the trapping voltage modulates the frequency of the axial motion, generating sidebands spaced by the modulation frequency ν_{mod}. ν_{mod} and the dc trapping voltage V_t can be adjusted to bring both the first upper sideband of N_2^+ and the first lower sideband of CO^+ within the bandwidth of the detector. When the axial motions of both ions are excited with a short pulse, the transient signals from the ions are simultaneously detectable (Fig. 3).

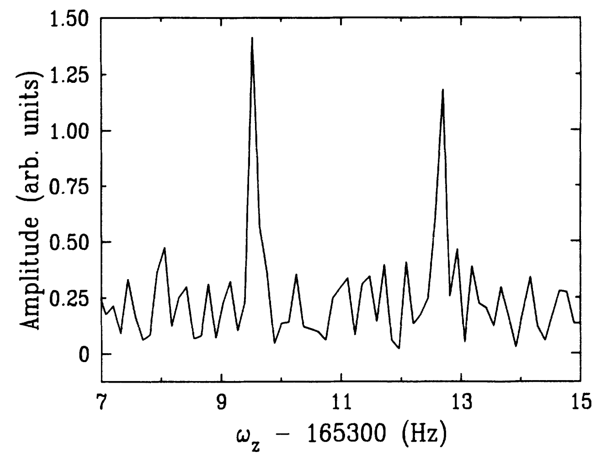

FIG. 3. The Fourier transform of the ring-down signal detected after the axial motions of trapped single CO^+ and N_2^+ ions are simultaneously excited. The trapping voltage is modulated at 15 Hz, giving rise to sidebands on the axial frequencies of the ions. Although the axial-frequency splitting of the ions is 33 Hz, the first upper sideband of the nitrogen ion and the first lower sideband of the carbon monoxide ion are separated by only 3 Hz and fall within the bandwidth of the axial motion detector. (A spurious peak, a fast-Fourier-transform artifact at 11 Hz, has been removed from the data.)

When both species of ion are in the trap, the observed axial frequencies differ from single-ion, unperturbed values. The qualitative nature of the shifts, a decrease of roughly 1 Hz for small excitations with the shift becoming less pronounced for larger axial orbits, agrees with the model described in Sec. II. A more quantitative comparison cannot be made with these data because at the time the data were recorded, there was an uncertainty in the overall calibration of orbit sizes (moreover, the trapping voltage was drifting in time). Even without good calibrations, however, there are several observations to be made.

First, the ion-ion perturbation is roughly constant in time. Over a period of 90 min, the axial-frequency shifts changed by less than 35%. Temporal drifts in the trapping voltage prevented setting a more stringent limit. Since the perturbations scale as ρ_s^{-3}, these data suggest that ρ_s varied by at most 10%.

Second, the perturbations, even though manifestly amplitude dependent, were quite symmetric. In Fig. 4 the ions have been pulsed to axial orbits larger than the radial separation. As the ions' axial motion damps, the effective coupling becomes stronger and the frequencies

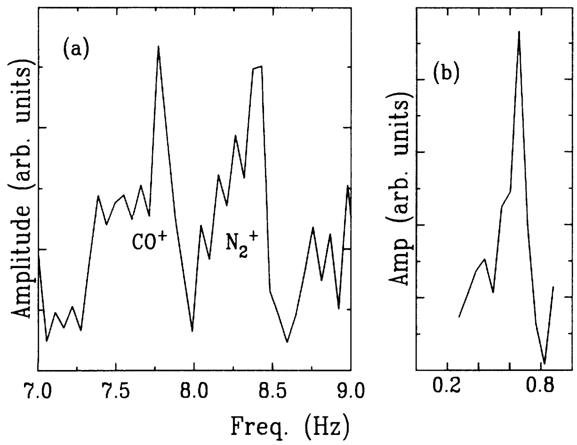

FIG. 4. The nonlinearity of the ion-ion interaction makes the axial-frequency perturbation amplitude dependent. (a) As the ions damp, their frequencies may shift over several of the Fourier-transform bin widths. In (b), we have transformed the signal shown in (a) to extract a signal at the difference frequency (see Ref. [16]). The sharpness of the feature in (b) is evidence that the difference frequency remains quite constant as the ions damp.

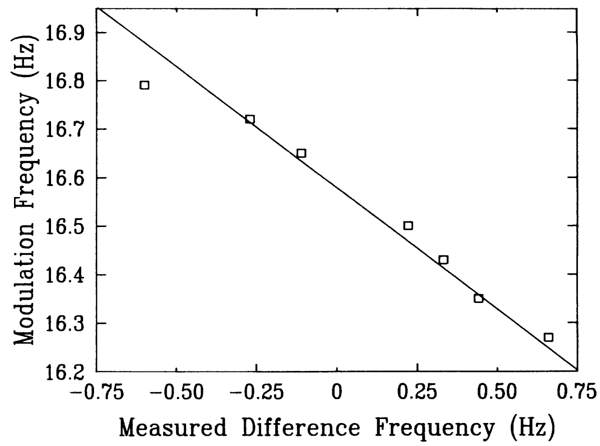

FIG. 5. The difference frequency between the two observed signals, $\delta\nu_z$, is measured for a variety of modulation frequencies $\nu_{\rm mod}$. Since we observe the first lower sideband of CO^+ and the first upper sideband of $N_2{}^+$, the difference between the frequencies of the actual axial motions is equal to $2\nu_{\rm mod}+\delta\nu_z$. The combined results: $\nu'_{z1}-\nu'_{z2}=33.14(3)$.

of both ions shift downward. This "chirp" in frequency is on the order of several Fourier-transform bin widths, and the transformed peaks look correspondingly messy. But since the shifts are identical, the difference in ion frequencies should remain constant, even as the individual frequencies shift. We numerically extract [16] from the data the difference frequency [Fig. 4(b)], which as expected is manifestly much more stable than either of the individual motions. The same numerical routine, incidentally, can extract a difference *phase* from the two chirped signals, which suggests a two-ion generalization of the phase-sensitive technique for measuring single-ion cyclotron frequencies described in Refs. [2] and [17].

Determining the axial-frequency splitting of a mass doublet is itself a mass measurement. Corrections due to magnetic field tilt and electrostatic anharmonicites are small and moreover should be identical for the two ions. Most important, temporal drifts in the trapping fields should not affect the measured mass ratio. Our measurement (Fig. 5) of

$$\omega_{z1}/\omega_{z2}=0.999\,799\,53(16)$$

corresponds to a mass ratio

$$M(CO^+)/M(N_2{}^+)=(\omega_{z1}/\omega_{z2})^2=0.999\,599\,1(3)\ ,$$

in agreement with published values [2,18]. Though an accuracy of 3 parts in 10^7 is not spectacular, attaining such an accuracy by comparing the *axial* mode frequencies illustrates the basic two-ion idea: Had we measured the axial frequency of a single CO^+ ion, dumped it out, loaded a single $N_2{}^+$ ion (a 30-min procedure), and measured *its* frequency, we should have been lucky to measure the mass ratio to even five times worse accuracy, given typical drifts in the axial frequency.

Of course, it is simultaneous measurement of *cyclotron*, not axial, frequencies that promises the ultimate high accuracy. The remainder of this paper addresses the question: How high can the accuracy be?

IV. MORE TWO-ION THEORY

A. Implication of the Brown and Gabrielse invariance theorem for two-ion measurements

All told, there are six normal modes for two ions in a Penning trap. We want to examine which of the six frequencies need be measured, to what accuracy, and how they should be combined in order to determine, to a part in 10^{11}, the ratio

$$R\equiv(m_1/m_2)=(1+\eta)/(1-\eta)=\omega_{c2}/\omega_{c1}\ . \qquad (4.1)$$

It turns out that for a mass doublet it is sufficient to measure only three frequencies, and of these only one, the trap cyclotron difference frequency $\Delta\omega'_c\equiv\omega'_{c1}-\omega'_{c2}$ need to be measured to a precision requiring two ions in the trap simultaneously.

Brown and Gabrielse have shown [19] that for a certain class of trapping-field imperfections (i.e., the quadrupole electric field not axially symmetric or magnetic field tilted with respect to the axis of the electric field), an invariance theorem relates the frequencies of motion in the trap to the free-space cyclotron frequency $\omega_c^2=(\omega'_c)^2+\omega_z^2+\omega_m^2$, where ω'_c, ω_z, and ω_m are the measured frequencies. The equality is true to all orders for a range of trap imperfections and provides a convenient prescription for combining the measured trap frequencies to recover the cyclotron frequency of the ion in a purely magnetic field. For two ions we write

$$\omega_{c1}^2=(\omega'_{c1})^2+\omega_{z1}^2+\omega_{m1}^2\ , \qquad (4.2a)$$

$$\omega_{c2}^2=(\omega'_{c2})^2+\omega_{z2}^2+\omega_{m2}^2\ , \qquad (4.2b)$$

where for the purposes of this section ω'_{ci}, ω_{zi}, and ω_{mi} refer to the frequencies of each ion as measured in the imperfect trap but unperturbed by ion-ion interaction.

Brown and Gabrielse [19] show that, for a single ion,

$$\omega_{z1}^2 \approx \frac{eV_t}{m_1 d^2}\left[1-\tfrac{3}{2}\sin^2\theta\left[1+\frac{\epsilon}{3}\cos(2\phi)\right]\right], \quad (4.3)$$

where ϵ specifies the out-of-roundness of the electric field and θ and ϕ the tilt angle of the magnetic field. For two particles of masses m_1 and m_2 in the same fields, we can approximate

$$\omega_{z2}^2 \approx R\,\omega_{z1}^2 . \quad (4.4)$$

How good is this approximation? For a typical mass doublet with mass less than 30 amu, and for reasonable trap parameters, the four quantities $(\omega_{z0}/\omega_{c0})^2$, η, $\sin^2\theta$, and ϵ are each less than 10^{-3}, so we ignore terms quartic in any combination of these four quantities. The error in Eq. (4.4), for example, is on the order of $\eta(\omega_{z0}/\omega_{c0})^2\sin^2\theta$, which contributes an error of order $\eta(\omega_{z0}/\omega_{c0})^4\sin^2\theta$ (less than 10^{-12}) to the final determination of R [Eq. (4.6)]. Consistent with an overall error of less than 10^{-12}, we may also approximate

$$\omega_{m2}^2 \approx \omega_{m1}^2 . \quad (4.5)$$

Using the approximations (4.4) and (4.5), we subtract Eq. (4.2a) from Eq. (4.2b) and solve for R:

$$R = \frac{\omega_{z1}^2}{2\omega_{c1}^2} + \left[1-\frac{\omega_{z1}^2}{2\omega_{c1}^2}\right]\left[1+\frac{(\Delta\omega_{c1}')(\Delta\omega_{c1}'-2\omega_{c1}')}{(\omega_{c1}-\omega_{z1}^2/2\omega_{c1})^2}\right]^{1/2} \quad (4.6)$$

and with no loss in accuracy at the part in 10^{12} level, we can replace ω_{c1}^2 in Eq. (4.6) with measured values:

$$\omega_{c1}^2 = (\omega_{c1}')^2 + \omega_{z1}^2 + (\omega_{z1}^2/2\omega_{c1}')^2 . \quad (4.7)$$

Thus to measure the mass ratio to a part in 10^{11}, it is sufficient to measure only three quantities, ω_{c1}', ω_{z1}, and $\Delta\omega_c' = \omega_{c1}' - \omega_{c2}'$. The first two quantities may be measured to relatively low accuracy, compared to the accuracy ultimately desired for R. The requisite precision for ω_{c1}' is lower than that desired for R by a factor of $(2\eta)^{-1}$, and for ω_{z1}, by a factor of $(2\eta)^{-1}(\omega_{c0}/\omega_{z0})^2$. At the level of a part in 10^8 for the cyclotron frequency and parts in 10^5 for the axial frequency, drifts in electric and magnetic fields are much less important, so in practice one can measure ω_{c1}' and ω_{z1} before putting the second ion in the trap, thereby ensuring that ion-ion interactions will not be a problem. $\Delta\omega_c'$ is extremely sensitive to drifts in the magnetic and electric fields, and thus must be measured with two ions in the trap.

This treatment in this subsection ignores ion-ion perturbation, spatial variation of the magnetic field, and nonquadrupole components of the electric field. Realistically, all these effects will be present. Their effects are addressed in the next two subsections.

B. Ion-Ion perturbation of the cyclotron frequency

As a first pass at the important question of ion-ion perturbation of the cyclotron difference frequency, we solve the set of linear differential equations approximate to the following idealized situation: The guiding centers of the cyclotron orbit of each ion are stationary, separated by ρ_s along the x axis. In this picture, there is no trap electric field, no time-averaged net force between the two ions, and the magnetic field is not B_0 but B_0'. The idea here is not to represent the trap realistically but rather to provide the simplest possible mathematical framework that still preserves the two-dimensionality of the ion-ion cyclotron coupling. If the cyclotron radii are small compared to ρ_s, we can approximate the interaction force as a linear function of ion displacements $\mathbf{r}_i$ from the guiding centers:

$$\mathbf{F}_1 = \frac{e^2(\mathbf{r}_1-\mathbf{r}_2+\rho_s\hat{\mathbf{x}})}{|\mathbf{r}_1-\mathbf{r}_2+\rho_s\hat{\mathbf{x}}|^3} - \frac{e^2\rho_s\hat{\mathbf{x}}}{\rho_s^3}$$
$$\approx -2m_0\Omega^2(x_1-x_2)\hat{\mathbf{x}} + m_0\Omega^2(y_1-y_2)\hat{\mathbf{y}} \quad (4.8)$$

and $\mathbf{F}_2 = -\mathbf{F}_1$. When we include the Lorentz force, we get a system of four linear differential equations for the motion of the two ions in two dimensions. Guessing solutions,

$$x_1 = \mathrm{Re}(A_{x1}e^{i\omega t}), \quad x_2 = \mathrm{Re}(A_{x2}e^{i\omega t}),$$
$$y_1 = \mathrm{Re}(A_{y1}e^{i\omega t}), \quad y_2 = \mathrm{Re}(A_{y2}e^{i\omega t}), \quad (4.9)$$

and solving the characteristic equation for ω, we get

$$\omega_1 = \omega_0/(1-\eta) + \Omega^2/(2\omega_0) + \Omega^4/(8\eta\omega_0^3) + O(\Omega^6(\eta^2\omega_0^5)),$$
$$\omega_2 = \omega_0/(1+\eta) + \Omega^2/(2\omega_0) - \Omega^4/(8\eta\omega_0^3) + O(\Omega^6/(\eta^2\omega_0^5)). \quad (4.10)$$

The answer is reassuring. The error in the all-important difference frequency $\delta(\omega_1-\omega_2)$ can be very small:

$$\delta(\omega_1-\omega_2)/\omega_0 = \Omega^4/(4\eta\omega_0^4) . \quad (4.11)$$

In our example of the two ammonia molecules, for $\rho_s = 0.10$ cm,

$$\delta(\omega_1-\omega_2)/\omega_0 = 10^{-14} .$$

But we must be careful. Although the perturbation in the difference frequency is small, the perturbation in either frequency alone is considerable. In the example just cited, $\delta\omega_i/\omega_0 = 2\times10^{-9}$. Thus if we aspire to a part in 10^{11} accuracy, we rely on the perturbation being symmetric to better than a percent. As we have seen, this is true in the case of linear coupling, but what if the cyclotron radii are large enough to be a non-negligible fraction of the ion separation? For coupling beyond the linear approximation, the size of the frequency perturbation will depend on the cyclotron radii, and if the cyclotron radii of the two ions are not exactly the same, we shall see that the ion-ion perturbations are *not* symmetric.

We will study the effect of nonlinear coupling using an approximation which keeps terms in the force expansion [Eq. (4.8)] out to order x_i^3, but which is in spirit lowest order in the coupling. At this level of approximation we treat the orbits as circular (that is, orbit shape is unperturbed; only frequency is recalculated) and treat the motions of the two ions as uncorrelated (that is, for the purpose of calculating the force on one ion, the other ion is imagined to be a thin ring of uniform charge density with radius ρ_{ci}). The force on ion 1 is

$$\begin{aligned}\mathbf{F}_1 \approx\, & m_0\Omega^2[-2x_1+3(x_1^2-\tfrac{1}{2}y_1^2+\tfrac{1}{4}\rho_{c2}^2)/\rho_s \\ & +(-3\rho_{c2}^2x_1-4x_1^3+6x_1y_1^2)/\rho_s^2]\hat{\mathbf{x}} \\ & +m_0\Omega^2[y_1-3x_1y_1/\rho_s+(\tfrac{3}{4}\rho_{c2}^2+6x_1^2y_1-\tfrac{3}{2}y_1^3)/\rho_s^2]\hat{\mathbf{y}}\end{aligned} \tag{4.12}$$

and similarly for ion 2. Using the unperturbed orbits to calculate the lowest-order perturbation to the fundamental frequencies, we get

$$\begin{aligned}\omega_1' &= \omega_0/(1-\eta)+\Omega^2/(2\omega_0)[1+(\tfrac{9}{4}\rho_{c1}^2+\tfrac{9}{8}\rho_{c2}^2)/\rho_s^2] \\ &\quad +O(\Omega^4/(\eta\omega_0^3)) \\ \omega_2' &= \omega_0/(1+\eta)+\Omega^2/(2\omega_0)[1+(\tfrac{9}{8}\rho_{c1}^2+\tfrac{9}{4}\rho_{c2}^2)/\rho_s^2] \\ &\quad +O(\Omega^4/(\eta\omega_0^3))\end{aligned} \tag{4.13}$$

and thus the error in the difference frequency is

$$\delta(\omega_1-\omega_2)/\omega_0=[9\Omega^2/(16\omega_0^2)][(\rho_{c1}^2-\rho_{c2}^2)/\rho_s^2] . \tag{4.14}$$

For reasonable experimental values of ρ_s, ρ_{c1}, and ρ_{c2}, the error due to nonlinear coupling [Eq. (4.14)] will be larger than the error due to purely linear frequency pulling [Eq. (4.11)]. We discuss the implications in Sec. V.

C. The magnetron motion when the ion masses are not equal

We shall show in this section that when the ion masses are not exactly the same, the average magnetron radii are not the same for the two ions. This difference in the average magnetron radii causes a systematic error in measuring the difference in the cyclotron frequencies if the trapping fields have spatial inhomogeneities that depend on the radial distance from trap center.

For ions of approximately equal mass, the conservation of energy and angular momentum [Eqs. (2.7) and (2.8)] severely constrain the range of possible paired-ion motion. The configuration which satisfies the conservation laws to first order in $\eta\omega_{mo}^2/\Omega^2$, shown in Fig. 6, is a modification of the degenerate mass orbit. The ions trace out twin circles on either side of the origin, and both circles themselves orbit the origin. As in the degenerate case, the centers of the circles are colinear with the origin, but in the nondegenerate case the distances from each circle's center to the origin differ from each other, and the radii of the circles are unequal as well. The distances s_i and c_i defined in Fig. 6, are given by

$$\begin{aligned} & s_1=\rho_s(1+\delta_{\rm mag})/2, \quad s_2=\rho_s(1-\delta_{\rm mag})/2 , \\ & c_1=\rho_{\rm com}(1-\delta_{\rm mag}), \quad c_2=\rho_{\rm com}(1+\delta_{\rm mag}) ,\end{aligned} \tag{4.15}$$

where $\delta_{\rm mag}=\eta\omega_{mo}^2/(2\Omega^2)$. As the mass difference η vanishes, $\rho_{\rm com}$ and ρ_s take on their original significance and

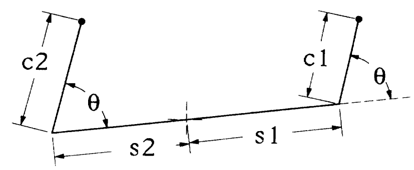

FIG. 6. Conservation laws dictate the allowed orbits for two trapped ions of unequal mass. To first order in $\eta\omega_{m0}^2/\Omega^2$, the pictured orbits conserve angular momentum and energy. By analogy with the degenerate mass limit [Fig. 2(b)], $\dot{\theta}$ is $\omega_s-\omega_{\rm com}$. In the nondegenerate case, $\dot{\theta}$ has a slight dependence on θ.

we recover the mass degenerate configuration shown in Fig. 2(b).

Errors from field imperfection are proportional to the time-averaged moments of the radii:

$$\langle\rho_i^n\rangle=\frac{\oint dt\,\rho_i^n}{\oint dt}=\frac{\int_0^{2\pi}d\theta(1/\dot{\theta})\rho_i^n}{\int_0^{2\pi}d\theta(1/\dot{\theta})} . \tag{4.16}$$

The instantaneous frequency difference between the two modes, $\dot{\theta}$, determines the rate at which the two ions take turns moving closer to and further from the center of the trap, and is basically a consequence, if viewed in a frame rotating with the common mode, of the *E*-cross-*B* drift induced by the interaction electric field. A simple estimate based on the separation between the ions, as determined from Fig. 6, and on the resulting $\mathbf{E}\times\mathbf{B}$ velocity, shows how $\dot{\theta}$ depends on θ:

$$\delta\theta/\theta=3(\rho_{\rm com}/\rho_s)(\eta\omega_{m0}^2/\Omega^2)\cos\theta . \tag{4.17}$$

To find the mean difference $\langle\rho_1^2-\rho_2^2\rangle$, the critical quantity in assessing the lowest-order error caused by nonideal fields, we evaluate the integral (4.16) for $n=2$:

$$\langle\rho_1^2-\rho_2^2\rangle=\left[\frac{\rho_s^2\omega_{m0}^2\eta}{2\Omega^2}\right]\left[1+O\left[\frac{\rho_{\rm com}}{\rho_s}\right]^2\right] . \tag{4.18}$$

As we shall see in Sec. V, the key result here is that the difference in the mean-square radii scales as ρ_s^2/Ω^2, that is, it scales as ρ_s^5.

V. AN ECONOMY OF ERRORS

In Sec. IV, when we applied the invariance theorem to two-ion measurements, we learned that part-per-10^{12} mass comparison requires three frequency measurements: two of single-ion frequencies and one of the two-ion cyclotron difference frequency. Errors affecting single-ion measurement have been thoroughly discussed elsewhere [16,20,21], so in this section we discuss only the various sources of error that affect the measurement of the crucial two-ion cyclotron difference frequency.

Sources of error in measuring $\Delta\omega_c'=\omega_{c1}'-\omega_{c2}'$ fall roughly into three categories. The first category consists of systematic errors having to do with field flaws and ion-ion perturbation. These errors scale as high powers of ρ_s and of $1/\rho_s$, respectively. In the second category are random errors associated with the measurement-to-measurement thermal fluctuations in the cyclotron radii. Into the third category we lump everything else, a hodgepodge of effects, all smaller than those in the first two categories.

A. Systematic errors associated with the magnetron motion

Assuming that we have cooled ρ_{com}, the scale of several of the largest sources of error is determined by ρ_s, the distances that magnetron mode-locking maintains between the guiding centers of the cyclotron motions. The ion-ion perturbation of $\Delta\omega_c'$ scales as $\Omega^4 \sim 1/\rho_s^6$ in the linear limit [Eq. (4.11)], and unequal cyclotron radii give rise to a nonlinear perturbation that scales as $\Omega^2/\rho_s^2 \sim 1/\rho_s^5$ [Eq. (4.14)]. On the other hand, the difference between the ions' mean-square distances from the center of the trap [Eq. (4.18)] scales as ρ_s^2/Ω^2, so errors in $\Delta\omega_c'$ due to field flaws scale as ρ_s^5 or higher power. Using Eqs. 10.15 and 10.18 from Ref. [20] and Eq. (4.18) above, we determine the averaged perturbation to the difference frequency from field flaws:

$$(\delta\Delta\omega_c'/\omega_c) = [-B_2/2 - \tfrac{3}{2}(\omega_{z0}^2/\omega_{c0}^2)C_4/d^2] \times [m_0\omega_{m0}^2\eta\rho_s^5/(2e^2)] , \quad (5.1)$$

where B_2 and C_4 are the lowest-order imperfections in the magnetic and electric fields, respectively, defined, for example, in Ref. [20].

If we measure the difference frequency several times, varying ρ_s, we an trace out the curve of measured $\Delta\omega_c'$ versus ρ_s. The high-power-law dependence on ρ_s and $1/\rho_s$ should be very distinctive (Fig. 7). The total error in $\Delta\omega_c'$ will be minimized by using a value measured along the flat section of the curve. Experimentally, an estimate of the residual error can be obtained by checking just how flat the curve is in the optimum region. As we reduce trapping-field imperfections, we can operate at larger values of ρ_s and reduce errors both from ion-ion interaction and from field gradients.

Suppose that an imbalance in the cyclotron drive electronics produces cyclotron radii which differ by 1% out of the mean radius of 0.019 cm. Suppose further that we have reduced the lowest-order field flaws until $|B_2| < 1\times10^{-7}/\text{cm}^2$ and $|C_4| < 2\times10^{-5}$.

Our laboratory experience leads us to believe these values are attainable [2,16]. Comparing the contributions to the error given by Eq. (4.14) and by Eq. (5.1), we find that the optimum separation will be around $\rho_s = 0.10$ cm (Fig. 7). The effects combined cause an error in the measured value of $\Delta\omega_c'/\omega_c$ of about 3×10^{-12}. There is a range of possible values of ρ_s, from 0.075 to 0.13 cm, for which the total error associated with the magnetron motion will be less than 7×10^{-12}.

The important point of this section is that errors which depend on the magnetron radius depend on it sharply. This remains true even if field flaws of higher order than B_2 and C_4 are dominant, and it remains true whether linear or nonlinear coupling causes the major error from ion-ion repulsion. In all cases the sharp divergence of the measured difference frequency at large and at small ion-ion separations will indicate the optimum operating regime and suggest the magnitude of the residual error.

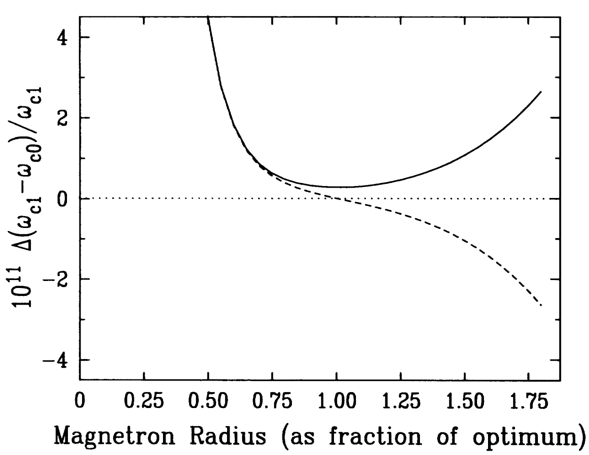

FIG. 7. Projected error in the measured value of $\omega_{c1}-\omega_{c2}$ as a function of ρ_s. Errors from ion-ion perturbation scale as ρ_s^{-5}, and errors from trapping-field flaws scale as ρ_s^5. In this example, B_2 and C_4 are the dominant field flaws and there is a systematic imbalance in the driven cyclotron radii of 1% out of an average cyclotron radius of 0.019 cm. The solid line corresponds to $B_2, C_4 < 0$ and the dotted line to $B_2, C_4 > 0$. The optimum value of the magnetron radius is defined here as the value of ρ_s at which the two sources of error make equal contributions. Experimentally, ρ_s can be varied in order to determine the region where the curve is relatively flat and the total error relatively small.

B. Thermal errors associated with the cyclotron radii

Field flaws, nonlinear ion-ion interaction, and special relativity all give the cyclotron frequency a dependence on the cyclotron radius ρ_c. In a trap tuned to the specifications mentioned above, the field flaw terms contributing to this dependence are relatively insignificant. The frequency corrections to the trap cyclotron difference frequency from special relativity and nonlinear interaction are

$$\delta(\Delta\omega_c'/\omega_{c0}) = [-\omega_{c0}^2/(2c^2) + 9\Omega^2/(16\omega_0^2\rho_s^2)](\rho_{c1}^2 - \rho_{c2}^2) . \quad (5.2)$$

Even if care is taken to ensure that the electronics that generate and deliver the rf pulses used to drive the cyclotron motion produce the same amplitude pulse at both frequencies, thermal errors will be troublesome. Residual thermal cyclotron motion will add randomly to the driven response, causing random and in general unequal fluctuations in the cyclotron radii. Although thermal effects will not shift the average measured difference frequency from its correct value, the fluctuations may be large enough to require an impractical number of measurements to obtain the desired overall precision.

For example, in our experiments the cyclotron motion is cooled to a $T_c = (\omega_c/\omega_z)T_z$, where T_z is the effective temperature of the resistance the axial motion sees—for our axial detector, $T_z = 4.2$ K. For our ammonia doublet, the cyclotron cooling limit corresponds to an rms cyclotron radius for each ion

$$(\langle \rho_{ci}^2 \rangle)^{1/2} = 0.0009 \text{ cm} .$$

With our existing detector sensitivity, we must drive the ions to $\rho_{ci} = 0.019$ cm to get the requisite signal-to-noise ratio to measure the difference frequency. At an ion-ion separation $\rho_s = 0.10$ cm, the dominant contribution to thermal fluctuations is from special relativity, at about 5 parts in 10^{11} per measurement. Since a single measurement with 5-parts-in-10^{11} resolution requires hundreds of seconds, averaging the thermal fluctuations to a part in 10^{11} would take hours of data collection. Clearly, efforts to improve detector sensitivity and cyclotron cooling methods will pay off.

C. Other perturbations at parts in 10^{12}

At parts-in-10^{12} accuracy, several little effects start to become significant. Among them are the following:

(i) Dipole-dipole interaction of the cyclotron motion with its image charge in the electrodes. Van Dyck *et al.* [22] have shown that, especially in small traps, this effect can be significant. For our larger trap with characteristic size $d = 0.55$ cm, this effect is on the order of two parts in 10^{11}, but should be the same for both ions to better than a part in 10^{12}.

(ii) Cyclotron frequency dependence on axial radius. Because we do not have to measure the axial frequency during a precision cyclotron measurement, the axial displacement can be very small—just the thermal value. The highest-precision, long-period measurements will span many thermal equilibration periods, so that both ions will have many opportunities to reequilibrate with the effective resistor in the axial motion detector, which will thoroughly average away any initial differences in thermal axial displacement the two ions might have.

(iii) Field changes caused by loading and purifying the ions. This effect may well cause shifts in the single-ion cyclotron frequency at the part-in-10^{10} level. But recall from Sec. IV the relative accuracies demanded of the three necessary frequencies. Our experience has been that loading and unloading ions from the trap does not cause any shift in the cyclotron frequency at the part-in-10^9 level, nor any shift in the axial frequency larger than a part in 10^5. Of course, any frequency change caused by loading or unloading ions is irrelevant to the simultaneous trap cyclotron difference frequency. Thus field changes caused by loading and purifying ions should cause no error in determination of the mass ratio to parts in 10^{12}.

VI. CONCLUSION

Our study of the the interacting motion of two simultaneously trapped ions supports the conclusion that temporal field drifts, special relativity, field imperfections, and ion-ion interaction pose no obstacles to part-in-10^{11} mass spectroscopy. Improvements in cyclotron cooling should bring part-in-10^{12} accuracy within reach. But no matter what one is trying to measure, attempting two-orders-of magnitude improvement in accuracy is likely to bring one up against unforeseen sources of error. Only experiment can be reassuring on this point.

ACKNOWLEDGMENTS

This work was supported by the NSF (Grant No. 8921769-PHY) and by the Joint Services Electronics Program (Grant No. DAAL03-89-C-0001). We thank A. Assmus for a critical reading of the manuscript and Frank DiFilippo for careful reading and helpful criticism.

*Present address: Joint Institute for Laboratory Astrophysics, Box 440, University of Colorado, Boulder, CO 80309.

†Present address: Department of Physics, Princeton University, Princeton, NJ 08544.

[1] R. S. Van Dyck Jr., F. L. Moore, D. L. Farnham, and P. B. Schwinberg, in *Frequency Standards and Metrology,* edited by A. DeMarchi (Springer-Verlag, Berlin, 1988), p. 349.

[2] E. A. Cornell, R. M. Weisskoff, K. R. Boyce, R. W. Flanangan, Jr., G. P. Lafyatis, and D. E. Pritchard, Phys. Rev. Lett. **63**, 1674 (1989).

[3] D. Hagena and G. Werth, Europhys Lett. **15**, 491 (1991).

[4] A program to determine the fine-structure constant independently from g-2 measurements (and without recourse to solid-state physics) will hinge on a one-part-in-10^{11} measurement of the mass ratio of two ammonia ions, $^{15}NH_3{}^+$ and $^{14}NDH_2{}^+$. Mass difference measurements, combined with γ-ray wavelength measurements, can determine the energy of a γ ray both in amu and in inverse centimeters. Twice the ratio of these two values, divided by the ratio of the mass of an electron in amu to the Rydberg in inverse centimeters, is α^2. An improved value for α, combined with improved electron g-2 measurements and calculations, will provide a more stringent test of quantum electrodynamics. See W. H. Johnson, in *Precision Measurements and Fundamental Constants II,* edited by B. N. Taylor and W. D. Phillips, Natl. Bur. Stand. (U.S.) Special Publication No. 617 (U.S. GPO, Washington, D.C., 1984), p. 335. See also Ref. [21].

[5] The electric field need not be inherently this stable if the axial frequency could be measured or locked to this accuracy. But axial damping and signal-to-noise limitations make such an axial-frequency measurement difficult.

[6] R. S. Van Dyck, Jr., F. L. Moore, D. L. Farnham, and P. B. Schwinberg, Rev. Sci. Instrum. **57**, 593 (1986).

[7] G. Gabrielse and J. Tan, J. Appl. Phys. **63**, 5143 (1988).

[8] H. G. Dehmelt, Adv. At. Mol. Phys. **3**, 53 (1967).

[9] Much of the theory of precision measurements with single ions in a Penning trap was developed at the University of Washington. For a comprehensive review of this work, see Ref. [20].

[10] D. J. Wineland, J. J. Bollinger, Wayne M. Itano, and J. D. Prestage, J. Opt. Soc. Am. B **2**, 1721 (1985).

[11] $\rho_s^2 = \rho_1^2 + \rho_2^2 - 2\boldsymbol{\rho}_1 \cdot \boldsymbol{\rho}_2$ constant implies $\boldsymbol{\rho}_1 \cdot \boldsymbol{\rho}_2$ constant. Therefore, $\rho_{\text{com}}^2 = \rho_1^2 + \rho_2^2 + 2\boldsymbol{\rho}_1 \cdot \boldsymbol{\rho}_2$ is constant.

[12] R. S. Van Dyck, Jr., P. B. Schwinberg, and H. Dehmelt, in *New Frontiers in High-Energy Physics,* edited by B. Kursunoglu, A. Perlmutter, and L. Scott (Plenum, New York, 1978), p. 159.

[13] D. J. Wineland and H. G. Dehmelt, Int. J. Mass Spectrosc. Ion Phys. **16**, 338 (1974); **19**, 251 (1975).

[14] A more detailed account of these experiments appears in

D. L. Kuchnir, undergraduate thesis, MIT, 1989.
[15] R. M. Weisskoff, G. P. Lafyatis, K. R. Boyce, E. A. Cornell, R. W. Flanagan, Jr., and D. E. Pritchard, J. Appl. Phys. **63**, 4599 (1988).
[16] E. A. Cornell, Ph.D. thesis, MIT, 1990.
[17] E. A. Cornell, R. M. Weisskoff, K. R. Boyce, and D. E. Pritchard, Phys. Rev. A **41**, 312 (1990).
[18] A. H. Wapstra and G. Audi, Nucl. Phys. A **432**, 1 (1985).
[19] L. Brown and G. Gabrielse, Phys. Rev. A **25**, 2423 (1982).
[20] L. Brown and G. Gabrielse, Rev. Mod. Phys. **58**, 233 (1986).
[21] F. L. Moore, Ph.D. thesis, University of Washington, 1989.
[22] R. S. Van Dyck, Jr., F. L. Moore, D. L. Farnham, and P. B. Schwinberg, Phys. Rev. A **40**, 6308 (1989).